

Dynamics of the Chain of Oscillators with Long-Range Interaction: From Synchronization to Chaos

G.M. Zaslavsky

*Courant Institute of Mathematical Sciences, New York University,
251 Mercer St., New York, NY 10012, USA
Department of Physics, New York University,
2-4 Washington Place, New York, NY 10003, USA*

M. Edelman

*Courant Institute of Mathematical Sciences, New York University,
251 Mercer St., New York, NY 10012, USA*

V.E. Tarasov

*Courant Institute of Mathematical Sciences, New York University,
251 Mercer St., New York, NY 10012, USA
Skobeltsyn Institute of Nuclear Physics,
Moscow State University, Moscow 119992, Russia*

(Dated: February 1, 2008)

Abstract

We consider a chain of nonlinear oscillators with long-range interaction of the type $1/l^{1+\alpha}$, where l is a distance between oscillators and $0 < \alpha < 2$. In the continuous limit the system's dynamics is described by the Ginzburg-Landau equation with complex coefficients. Such a system has a new parameter α that is responsible for the complexity of the medium and that strongly influences possible regimes of the dynamics. We study different spatial-temporal patterns of the dynamics depending on α and show transitions from synchronization of the motion to broad-spectrum oscillations and to chaos.

A chain of nonlinear interacting oscillators is a model of the wide-spread investigation of different physical phenomena such as synchronized behavior of the system, bifurcations to different regimes, spatial-temporal turbulent or chaotic dynamics, different instabilities, appearance of defects, and many others. The long range interaction between oscillators leads to a new qualitative dynamics and thermodynamics. Our consideration is related to the power-law long-range interaction that makes it possible to find new regimes of the system and to establish a link of the corresponding equations of motion to the equations with fractional derivatives.

I. INTRODUCTION

The goal of the paper is to consider different dynamical regimes, from synchronization to chaos and turbulence, in a chain of large number of coupled nonlinear oscillators with long-range interaction (LRI) of a power type. The potential of interaction is nonlocal and proportional to $1/l^{1+\alpha}$ with l as a distance between oscillators and $0 < \alpha < 2$, ($\alpha \neq 1$). It will be called α -interaction. Transitions between different regimes of the chain behavior are considered as a function of α . In the continuous limit the system reduces to the fractional generalization of the Ginzburg-Landau (FGL) equation and the chain of oscillators can be considered as a discretized model of FGL, called DFGL. Since we also consider the model with complex coefficients, it either can be related to a fractional generalization of the complex nonlinear Schrödinger equation.

The literature related to this type of problem is fairly vast and we would refer only to some reviews and closely related articles. The complex Ginzburg-Landau (CGL) equation is typically considered for pattern formation in different media [1, 2, 3]. CGL equation appears in numerous physical models (see for example [4, 5, 6, 7]). Long-range interaction with finite radius of interaction was considered for complex media in [8, 9] and for the α -interaction in [10, 11, 12, 13, 14]. Different regimes of synchronization in the chain of coupled oscillators with nearest neighbour interaction can be found in reviews [15, 16] while the synchronization with α -interaction for DFGL was found in [17, 18]. The FGL equation was introduced in [19] to describe the wave propagation in complex media, when the dispersion law has fractional power of the wave number. The related case appears in description of weak turbulence [20].

More examples related to the chains with LRI and their solution and breather type solutions and applications can be found in [21, 22].

The main part of this paper is a numerical simulation of the chain of $N = 512$ coupled oscillators with α -interaction and constant external force that pump energy into the system. This system links to the FGL equation in continuous limit based on the formal procedure introduced in [17, 23].

It will be shown that the forcing oscillatory media with LRI exhibits transition to chaos and turbulence when α decreases. As another interesting regime, we found a "collectivized" limit cycle that has a broad spectrum in phase space of any individual oscillator. Such a cycle exists within an interval of α .

In Sec. 2, we present the basic equation for coupled oscillators and their continuous media limit. This part includes some modified version of the results of [17, 24]. In Sec. 3, we consider fractional generalization of the CGL equation and some of its stability criteria. The Secs 4-6 play an auxiliary role to identify an interesting domain of parameters to be studied. The main numerical results are presented in Secs. 7-9. It is important to note that the main studied object is the chain of nonlinear oscillators, and a part of the obtained results can be appropriate for the complex FGL equation at least for a finite time. The FGL equation can also be used for some estimates of the critical parameters to change the regimes of behavior of the chain of oscillators.

II. CHAIN OF OSCILLATORS WITH LONG-RANGE INTERACTION

Following [24], let us introduce the system by its action

$$S[Z_n] = \int_{-\infty}^{+\infty} dt \left(\sum_{n=-\infty}^{+\infty} \left[\frac{1}{2} \dot{Z}_n(t) \dot{Z}_n(t) - V(Z_n(t)) \right] - \sum_{\substack{n,m=-\infty \\ m \neq n}}^{+\infty} U(Z_n(t), Z_m(t)) \right), \quad (1)$$

where Z_n are displacements of the oscillators from their equilibrium, and $U(Z_n(t), Z_m(t))$ is defined by

$$U(Z_n(t), Z_m(t)) = \frac{1}{4} g_0 J_\alpha(|n - m|) (Z_n(t) - Z_m(t))^2, \quad (n \neq m) \quad (2)$$

with g_0 as an interaction constant, and with interparticle interaction

$$J_\alpha(|n - m|) = \frac{1}{|n - m|^{\alpha+1}}, \quad (\alpha > 0). \quad (3)$$

The usual linear oscillator term $Z_n^2(t)$ can be included into $V(Z_n(t))$. The corresponding Euler-Lagrange equations are

$$\frac{dZ_n}{dt} + g_0 \sum_{\substack{m=-\infty \\ m \neq n}}^{+\infty} J_\alpha(|n-m|) [Z_m(t) - Z_n(t)] + F(Z_n(t)) = 0, \quad (4)$$

where $F(u) = \partial V(u)/\partial u$.

Continuous limit of equation (4) can be defined by a transform operation from $Z_n(t)$ to $Z(x, t)$ [17, 23]. Firstly, define $Z_n(t)$ as Fourier coefficients of some function $\hat{Z}(k, t)$, $k \in [-K_0/2, K_0/2]$, i.e.

$$\hat{Z}(t, k) = \sum_{n=-\infty}^{+\infty} Z_n(t) e^{-ikx_n} = \mathcal{F}_\Delta\{Z_n(t)\}, \quad (5)$$

where $x_n = n\Delta x$, and $\Delta x = 2\pi/K_0$ is a distance between nearest particles in the chain, and

$$Z_n(t) = \frac{1}{K_0} \int_{-K_0/2}^{+K_0/2} dk \hat{Z}(t, k) e^{ikx_n} = \mathcal{F}_\Delta^{-1}\{\hat{Z}(t, k)\}. \quad (6)$$

Secondly, in the limit $\Delta x \rightarrow 0$ ($K_0 \rightarrow \infty$) replace $Z_n(t) = (2\pi/K_0)Z(x_n, t) \rightarrow Z(x, t)dx$, and $x_n = n\Delta x = 2\pi n/K_0 \rightarrow x$. In this limit, Eqs. (5), (6) are transformed into the integrals

$$\tilde{Z}(t, k) = \int_{-\infty}^{+\infty} dx e^{-ikx} Z(t, x) = \mathcal{F}\{Z(t, x)\} = \lim_{\Delta x \rightarrow 0} \mathcal{F}_\Delta\{Z_n(t)\}, \quad (7)$$

$$Z(t, x) = \frac{1}{2\pi} \int_{-\infty}^{+\infty} dk e^{ikx} \tilde{Z}(t, k) = \mathcal{F}^{-1}\{\tilde{Z}(t, k)\} = \lim_{\Delta x \rightarrow 0} \mathcal{F}_\Delta^{-1}\{\hat{Z}(t, k)\}. \quad (8)$$

Applying (5) to (4) and performing the limit (7), we obtain

$$\frac{\partial Z(t, x)}{\partial t} + g_\alpha \frac{\partial^\alpha Z(t, x)}{\partial |x|^\alpha} + F(Z(t, x)) = 0, \quad (1 < \alpha < 2), \quad (9)$$

where $\partial^\alpha/\partial |x|^\alpha$ is the fractional Riesz derivative [25] defined by

$$\frac{\partial^\alpha Z(t, x)}{\partial |x|^\alpha} = \mathcal{F}^{-1}\{|k|^\alpha \tilde{Z}(t, k)\},$$

and

$$g_\alpha = 2g_0(\Delta x)^\alpha \Gamma(-\alpha) \cos\left(\frac{\pi\alpha}{2}\right) \quad (10)$$

is the renormalized interaction constant. Equations of type (9) with different nonlinear terms were considered in [17, 23]. For other values of α one can obtain similar equation to (9) by performing the corresponding transform operation.

III. COMPLEX NONSTATIONARY GINZBURG-LANDAU EQUATION

Consider a chain of the nearest-neighbour coupled nonlinear oscillators described by the equations

$$\frac{d}{dt}Z_n(t) = (1 + ia)Z_n - (1 + ib)|Z_n|^2Z_n + (c_1 + ic_2)(Z_{n+1} - 2Z_n + Z_{n-1}), \quad (11)$$

where we assume that all oscillators have the same internal parameters. Such equations can be obtained from (4) for $\alpha = \infty$ and the corresponding choice of g_0 and $V(Z_n)$. Transition to the continuous medium assumes that the difference $Z_{n+1} - Z_n$ is of the same order as Δx , and the interaction constants c_1 and c_2 are fairly large. Setting $c_1 = g(\Delta x)^{-2}$, $c_2 = gc(\Delta x)^{-2}$ with new constants g and c , we get

$$\frac{\partial}{\partial t}Z = (1 + ia)Z - (1 + ib)|Z|^2Z + g(1 + ic)\frac{\partial^2}{\partial x^2}Z, \quad (12)$$

which is a time-dependent complex Ginzburg-Landau (CGL) equation.

Let us come back to the equation for nonlinear oscillators with fractional long-range coupling

$$\frac{d}{dt}Z_n = (1 + ia)Z_n - (1 + ib)|Z_n|^2Z_n + g_0 \sum_{m \neq n} \frac{1}{|n - m|^{\alpha+1}}(Z_n - Z_m), \quad (13)$$

where $Z_n = Z_n(t)$ is the position of the n -th oscillator in the complex plane, $1 < \alpha < 2$, and the corresponding choice of $F(Z_n) = (1 + i\alpha)Z_n - (1 + ib)|Z_n|^2Z_n$ has been done. The corresponding equation in the continuous limit is

$$\frac{\partial}{\partial t}Z = (1 + ia)Z - (1 + ib)|Z|^2Z + g(1 + ic)\frac{\partial^\alpha}{\partial |x|^\alpha}Z, \quad (1 < \alpha < 2, \quad \alpha \neq 1) \quad (14)$$

where $g(1 + ic) = g_0 a_\alpha$,

$$a_\alpha = 2\Gamma(-\alpha) \cos(\pi\alpha/2). \quad (15)$$

Eq. (14) is a fractional generalization of the complex nonstationary Ginzburg-Landau (FGL) equation (12). Equation (13) is the same as (4) with a special choice of V . It was suggested in [19] to describe complex media with fractional dispersion law.

The FGL equation (14) can be presented as the system of real equations

$$\frac{d}{dt}X = \left(1 - g\frac{\partial^\alpha}{\partial |x|^\alpha}\right)X - \left(a - gc\frac{\partial^\alpha}{\partial |x|^\alpha}\right)Y - (X^2 + Y^2)(X - bY),$$

$$\frac{d}{dt}Y = \left(1 - g\frac{\partial^\alpha}{\partial|x|^\alpha}\right)Y + \left(a - gc\frac{\partial^\alpha}{\partial|x|^\alpha}\right)X - (X^2 + Y^2)(Y + bX), \quad (16)$$

where $X = X(t, x)$ and $Y = Y(t, x)$ are real and imaginary parts of $Z(t, x)$.

The results of numerical simulation of the system (13) can be applied for a finite time for the FGL equation (14) although it is well known that typically the discrete systems are more chaotic than their continuous counterpart. The system (13) will be called discretized FGL equation or simply DFGL.

IV. PARAMETERS OF STABILITY OF PLANE-WAVE SOLUTION

In this section, we obtain some conditions of instability that will be implemented in numerical simulations of the system (13). These conditions are easy to derive and interpret considering the FGL equation.

To obtain a particular solution of the FGL equation (14) with a fixed wave number K , we consider Z in the form

$$Z(x, t) = A(K, t)e^{iKx}. \quad (17)$$

Substitution of (17) into (14) gives

$$\frac{\partial}{\partial t}A(K, t) = (1 + ia)A - (1 + ib)|A|^2A - g(1 + ic)|K|^\alpha A. \quad (18)$$

The plane-wave solution of (18) is

$$A(x, t) = (1 - g|K|^\alpha)^{1/2}e^{iKx - i\omega_\alpha(K)t}, \quad 1 - g|K|^\alpha > 0, \quad (19)$$

where

$$\omega_\alpha(K) = (b - a) + (c - b)g|K|^\alpha, \quad 1 - g|K|^\alpha > 0. \quad (20)$$

Solution of (19) can be presented as

$$\begin{aligned} X_0(x, t) &= (1 - g|K|^\alpha)^{1/2} \cos(Kx - \omega_\alpha(K)t + \theta_0), \\ Y_0(x, t) &= (1 - g|K|^\alpha)^{1/2} \sin(Kx - \omega_\alpha(K)t + \theta_0), \quad 1 - g|K|^\alpha > 0, \end{aligned} \quad (21)$$

where $X = X(x, t) = \text{Re}Z(x, t)$, $Y = Y(x, t) = \text{Im}Z(x, t)$, and θ_0 is an arbitrary constant phase. These solution can be interpreted as synchronized state of the oscillatory medium. In fact, it will be shown by simulation that the synchronized solution exists also for the DFGL equation (13).

To obtain the stability condition, consider the variation of (18) near solution (21):

$$\frac{d}{dt}\delta X = A_{11}\delta X + A_{12}\delta Y, \quad \frac{d}{dt}\delta Y = A_{21}\delta X + A_{22}\delta Y, \quad (22)$$

where δX and δY are small variations of X and Y , and

$$\begin{aligned} A_{11} &= 1 - g|K|^\alpha - 2X_0(X_0 - bY_0) - (X_0^2 + Y_0^2), \\ A_{12} &= -a + gc|K|^\alpha - 2Y_0(X_0 - bY_0) + b(X_0^2 + Y_0^2), \\ A_{21} &= a - gc|K|^\alpha - 2X_0(Y_0 + bX_0) - b(X_0^2 + Y_0^2), \\ A_{22} &= 1 - g|K|^\alpha - 2Y_0(Y_0 + bX_0) - (X_0^2 + Y_0^2). \end{aligned} \quad (23)$$

The conditions of asymptotic stability for (22) are

$$A_{11} + A_{22} < 0, \quad A_{11}A_{22} - A_{12}A_{21} < 0. \quad (24)$$

Substitution of Eqs. (21) and (23) into (24) gives

$$A_{11} + A_{22} = -2(1 - g|K|^\alpha), \quad (25)$$

$$A_{11}A_{22} - A_{12}A_{21} = \left(b(1 - g|K|^\alpha) - (a - gc|K|^\alpha)\right)\left(3b(1 - g|K|^\alpha) - (a - gc|K|^\alpha)\right). \quad (26)$$

Then the conditions (24) have the form

$$1 - g|K|^\alpha > 0,$$

$$1 - g|K|^\alpha < a/b - (c/b)g|K|^\alpha < 3(1 - g|K|^\alpha), \quad (27)$$

i.e. the plane-wave solution (19) is unstable if the parameters a , b , c and g do not satisfy (27).

Condition (27) defines the region of parameters for plane waves where the synchronization can exist.

In the numerical simulation, we use the parameters

$$a = -1.2, \quad b = -2, \quad c = 2, \quad g = 1. \quad (28)$$

Then Eq. (27) gives the inequalities

$$0 < 1 - |K|^\alpha < 0.6 + |K|^\alpha < 3(1 - |K|^\alpha). \quad (29)$$

As a result, the plane-wave solution with $E = 0$ is stable for

$$0.2 < |K|^\alpha < 0.6, \quad (1 < \alpha < 2). \quad (30)$$

In our numerical simulation, we use the initial conditions with

$$|K| = 2\pi/64 \approx 0.09817 \quad (31)$$

that is K is in the unstable region for $1 < \alpha < 2$. In the following the initial conditions with perturbation $E \neq 0$ will be out of the boundaries (30), and evolution of the initially unstable states will be studied.

V. MAPPING THE NUMERICAL DATA

Numerical results are obtained as solutions of the coupled equations

$$\frac{d}{dt}Z_n = (1 + ia)Z_n - (1 + ib)|Z_n|^2Z_n + \frac{1 + ic}{a_\alpha(\Delta x)^\alpha} \sum_{m \neq n}^N \frac{1}{|n - m|^{\alpha+1}}(Z_n - Z_m) + E, \quad (32)$$

where $n = 1, \dots, N$, $\Delta x = 1$, and E is a constant external force. In simulations, the number of oscillators was $N = 512$, and the external force was $E = 0.3$. In the continuous limit, Eq. (32) transforms into the FGL equation with forcing.

For all sets of parameters, we integrate the DFGL equations with the initial conditions

$$Z_n(0) = A_0 e^{iK_n}, \quad (33)$$

where $|K| = 2\pi/T$, the space period is $T = 64$, and A_0 is an initial amplitude. Numerical solutions were stored at each $t_q = 0.005q$, where $q \in \mathbb{N}$.

To visualize the numerical solution we consider the following values.

(1) We plot the surface $|Z(x, t)|^2$ and the phase-space projection of the central oscillator ($n = 0, x_n = 0$) formed by the variables:

$$A(t) = |Z(0, t)|^2, \quad \dot{A}(t) = \frac{dA(t)}{dt}. \quad (34)$$

(2) In addition to (34), we plot $Y(t) = \text{Im}(Z(0, t))$ vs. $X(t) = \text{Re}(Z(0, t))$ for better resolution of the central oscillator behavior.

(3) We calculate the discrete Fourier transform of the sequence $Z(0, t_q)$ defined as

$$\hat{Z}_n(\omega_j) = \frac{1}{Q} \sum_{q=0}^{Q-1} Z_n(t_q) \exp(-i \omega_j t_q), \quad (35)$$

$$Z_n(t_q) = \sum_{j=0}^{Q-1} \hat{Z}_n(\omega_j) \exp(i \omega_j t_n), \quad (36)$$

where $\omega_j = 2\pi j/Q$, ($j = 0, \dots, Q-1$). The power spectrum S of the sequence $Z_n(t_q)$ for $q = 0, \dots, Q-1$ is given by

$$S_j \equiv S(\omega_j) = |\hat{Z}_n(\omega_j)|^2. \quad (37)$$

Our main goal is to compare solutions of the DFGL equation for different values of $\alpha \in (1, 2)$ and consider emergence of chaotic dynamics of the chain of oscillators as a function of α . The larger is α , the weaker is long-range interaction.

In the simulations, we consider the following plots.

- (a) Color plots present surfaces $|Z_n(t)|^2$ vs t and n ;
- (b) Plane $(A, dA/dt)$ displays a projection of the trajectory of the central oscillator (see definition in (34));
- (c) Plane $(\text{Re } Z, \text{Im } Z)$ displays a projection of the complex amplitude $Z = Z(0, t)$ of the central oscillator as a function of time;
- (d) Plots $(\log_{10} \omega, \log_{10} S)$ describe the spectrum of time oscillations of $Z(0, t)$ (see definition in Eq. (37)).

VI. SOME NUMERICAL RESULTS FOR CGL EQUATION

In this section, we provide some numerical results derived in [17, 26, 27, 28, 29] for the complex Ginzburg-Landau (CGL) equation in order to compare them, obtained for $\alpha = 2$, with our results for $\alpha < 2$. For many other results and details see [1, 3, 15].

- (a) In paper [27], the CGL equation has been considered for the parameters

$$\alpha = 2, \quad a = 0 \quad b = 1.333, \quad c = -1. \quad (38)$$

and the phase turbulence has been observed.

- (b) It was shown in [28] that for the parameters

$$\alpha = 2, \quad a = 0, \quad b = -1.4, \quad c = 0.6 \quad (39)$$

solution of the CGL equation has chaotic states and it is spatial-temporal intermittent.

- (c) It was found in [28] that for the parameters

$$\alpha = 2, \quad a = 0, \quad b = 1.2, \quad c = -0.6 \quad (40)$$

solution of the CGL equation has zigzagging holes near the transition to the plane waves.

(d) In [26], the CGL equation was considered for the parameters

$$\alpha = 2, \quad a = -1.2, \quad b = -2, \quad c = 2. \quad (41)$$

For $E = 0.35$ the solution displays pitchforks without defects while for $E = 0.23$ the rare defects were observed.

(e) In [17], the FGL equation was considered for the parameters

$$1 < \alpha < 2, \quad a = 1, \quad b = 0, \quad c = 70. \quad (42)$$

It was shown that the solution had one stable fixed point for $\alpha_0 < \alpha < 2$, ($\alpha_0 = 1.51$) that corresponds to synchronization of oscillators. Decreasing of α below α_0 leads to a limit cycle via the Hopf bifurcation.

VII. TRANSITION FROM SYNCHRONIZATION TO TURBULENCE

Regular propagation in time of the initial state of the chain of oscillators will be called synchronization. To consider α -dependence of transition from synchronization to turbulence near $\alpha = 2$, we use the parameters

$$a = -1.2, \quad b = -2, \quad c = 2, \quad A_0 = 0.2, \quad (43)$$

similar to (41) that were used in [26] for the CGL equation (14), but for the chain of oscillators with $\alpha \neq 2$. The simulation was performed for the chain of 512 oscillators with parameters equivalent to (43).

In Fig.1., the surfaces of $|Z_n(t)|^2$ vs t and $x = n$ for $\alpha = 1.940$, $\alpha = 1.935$, $\alpha = 1.930$, $\alpha = 1.925$, $\alpha = 1.910$, $\alpha = 1.810$ are shown. For $\alpha = 1.940$, we have a regular space structure of the plane-wave type. For $\alpha = 1.935$, there is a space modulation, which deforms the regular space structure. For $\alpha = 1.930$, we can see the appearance of defects and pitchforks. For $\alpha = 1.925$, the structure in the space-time demonstrates sharp and drastic changes. There exist many defects and pitchforks. For $\alpha = 1.910$, the number of defects and pitchforks is increased, and some pitchforks are joined. For $\alpha = 1.810$, we can see chaos and turbulence, and synchronization is completely lost. We see that the amplitude turbulence

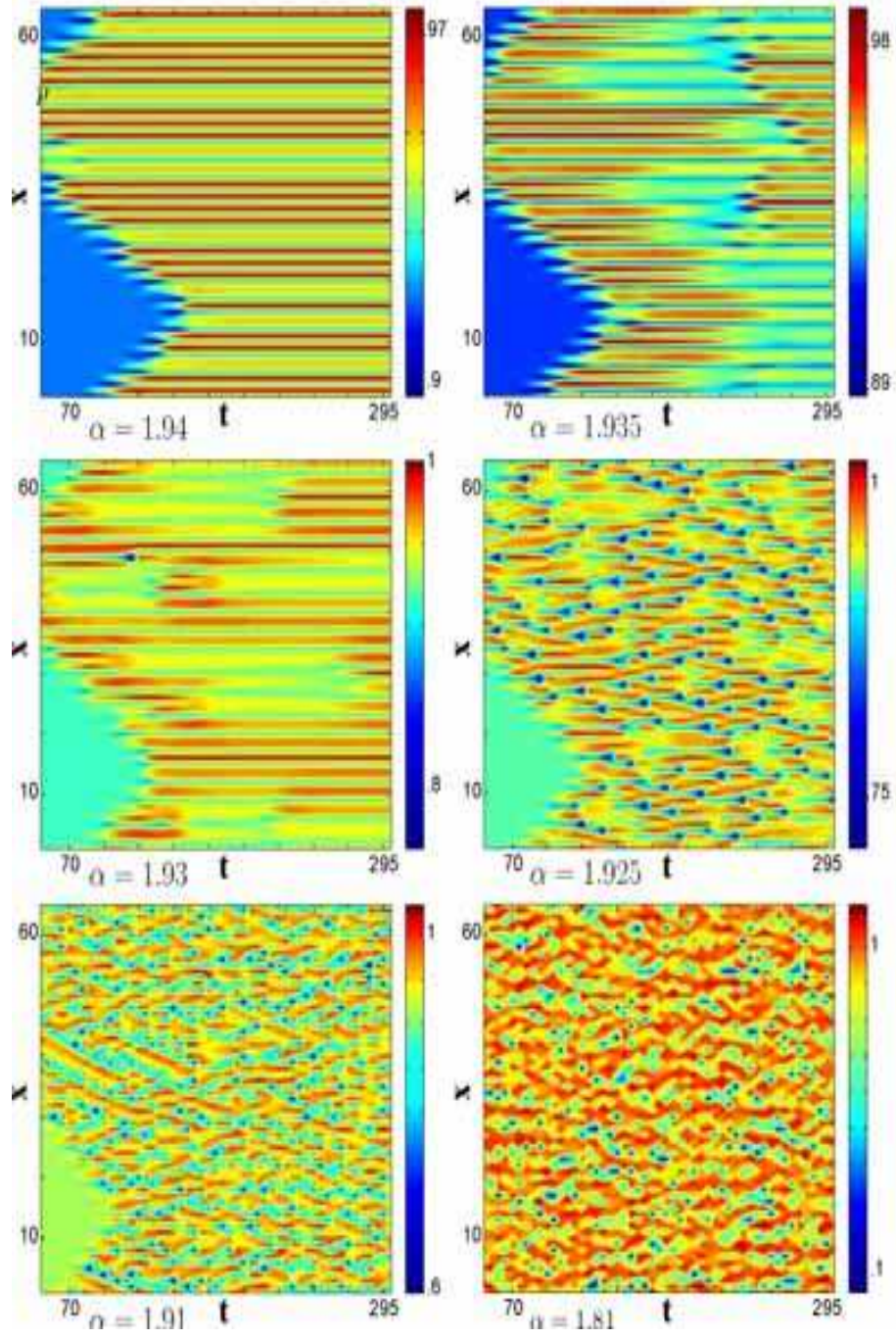


FIG. 1: Alpha-dependence of transition from synchronization to turbulence near $\alpha = 2$. Surfaces of $|Z_n(t)|^2$ vs t and $x = n$ for $\alpha = 1.940$, $\alpha = 1.935$, $\alpha = 1.930$, $\alpha = 1.925$, $\alpha = 1.910$, $\alpha = 1.810$. Simulations are realized for FGL equation with parameters $a = -1.2$, $b = -2$, $c = 2$, $A_0 = 0.2$.

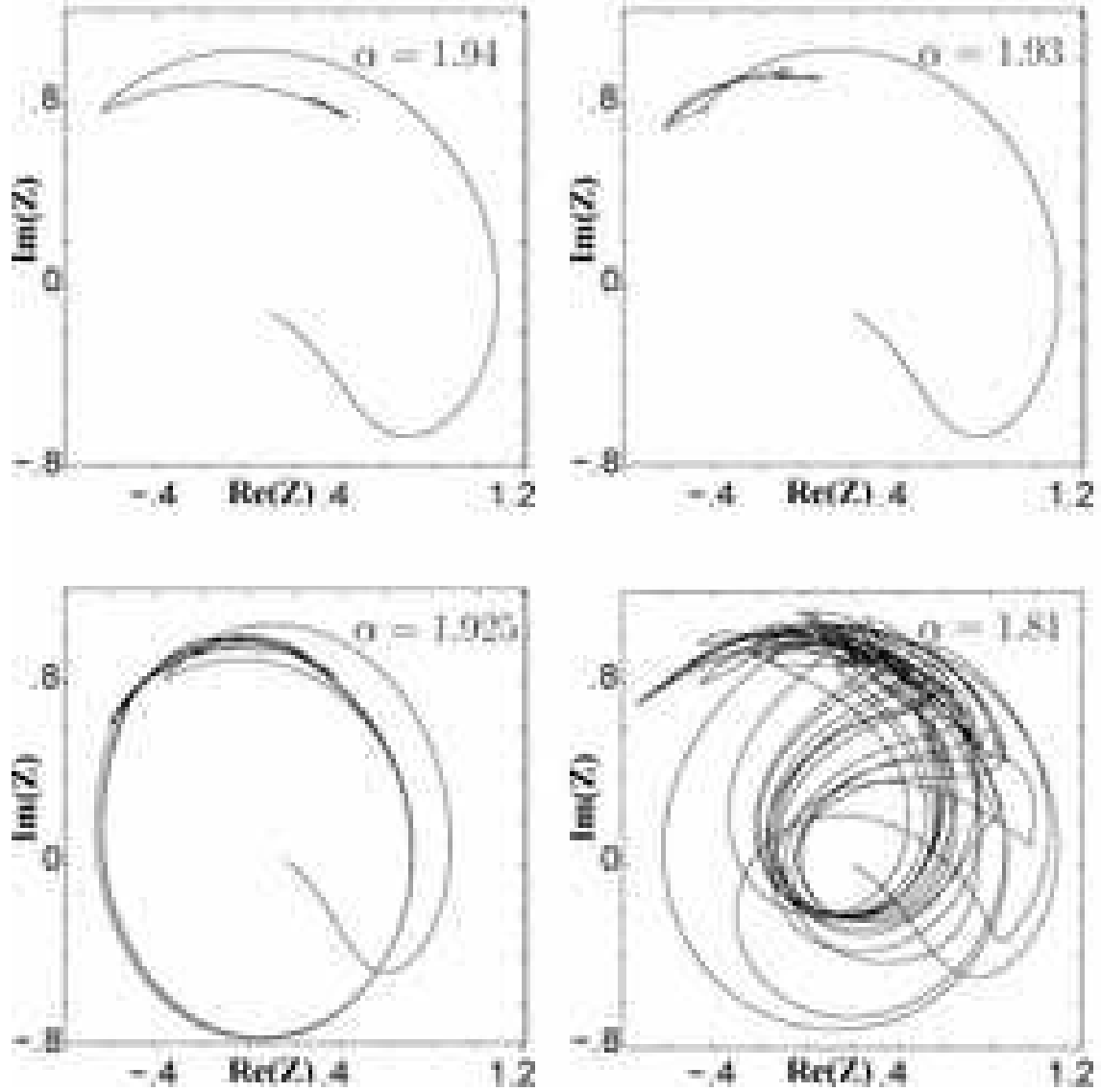


FIG. 2: Alpha-dependence of transition from synchronization to turbulence near $\alpha = 2$. Plane $(\text{Re } Z, \text{Im } Z)$ shows projection of the complex amplitude $Z = Z(0, t)$ of the central oscillator as a function of time for $\alpha = 1.940$, $\alpha = 1.930$, $\alpha = 1.925$, $\alpha = 1.810$.

is characterized by persistent creation and annihilation of pitchforks. The decreasing of order of fractional derivative means increasing a role of LRI. It is worthwhile to comment that the loss of synchronization and the emergence of amplitude turbulence is fairly sharp with fairly small change of α .

In Fig.2., the plane $(\text{Re } Z, \text{Im } Z)$ shows projection of the complex amplitude $Z = Z(0, t)$ of the central oscillator as a function of time for $\alpha = 1.940$, $\alpha = 1.930$, $\alpha = 1.925$, $\alpha =$

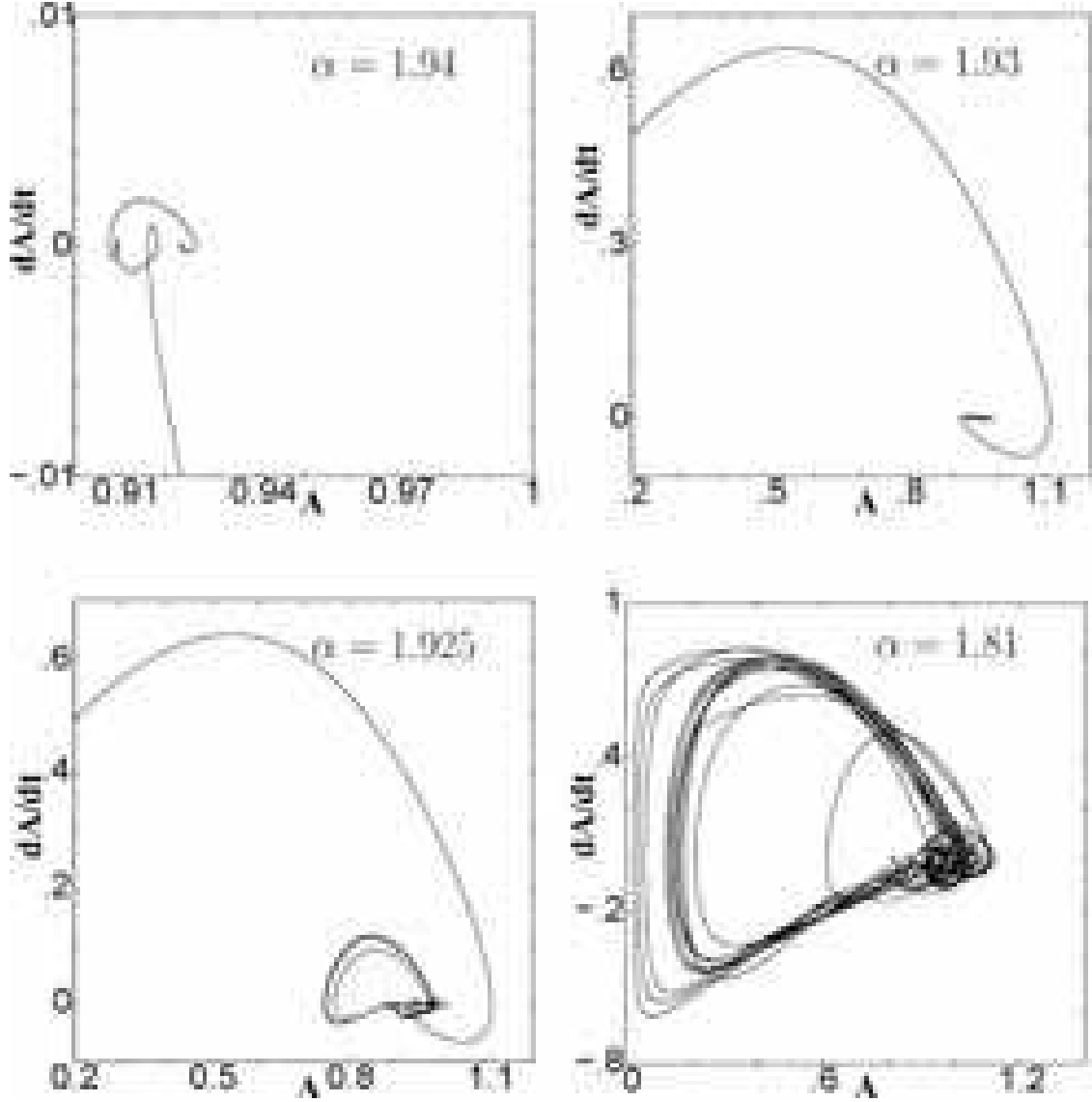


FIG. 3: Alpha-dependence of transition from synchronization to turbulence near $\alpha = 2$. Plane $(A, dA/dt)$ shows projection of the trajectory of the central oscillator in phase space, where $A(t) = |Z(0, t)|^2$ for $\alpha = 1.940$, $\alpha = 1.930$, $\alpha = 1.925$, $\alpha = 1.810$.

1.810. For $\alpha = 1.94$ and $\alpha = 1.93$, there is a stable node, which means the existence of synchronization. Confirmation of that can also be found in Fig.3, where

the plane $(A, dA/dt)$ shows projection of the trajectory of the central oscillator and $A(t) = |Z(0, t)|^2$. For $\alpha = 1.94$ and $\alpha = 1.93$, the attracting point that corresponds to synchronization of the chain of oscillators is clearly seen. Characteristics of the turbulent motion, shown in Fig.1. for $\alpha = 1.925$, $\alpha = 1.91$, $\alpha = 1.81$, are different from the cases of larger α . This difference can be better recognized from the Figs.2-4. Particularly, in Fig.2.

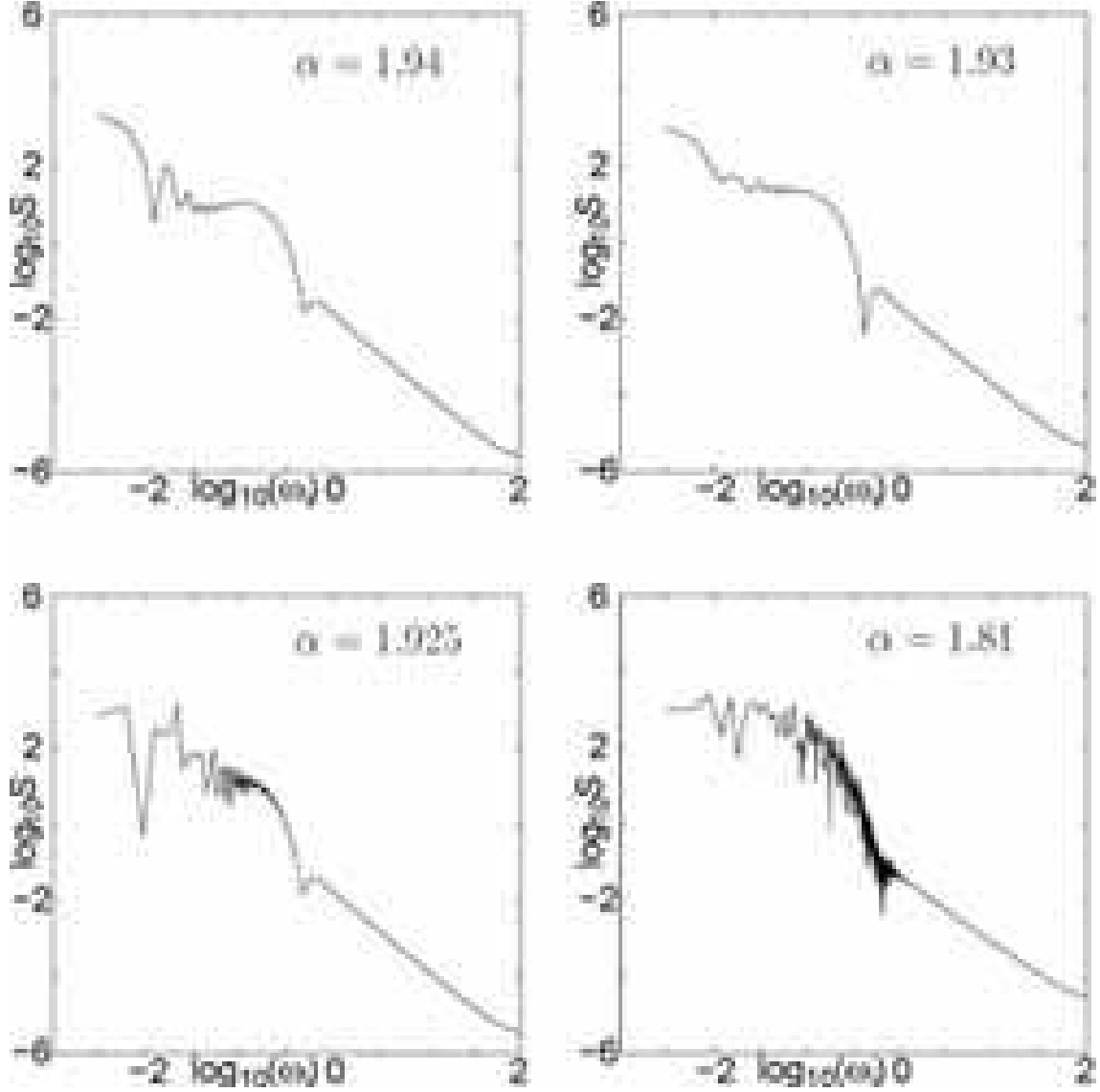


FIG. 4: Alpha-dependence of transition from synchronization to turbulence near $\alpha = 2$. Spectrum of time oscillations of $Z(0, t)$ (see definition in Eq. (37)) for $\alpha = 1.940$, $\alpha = 1.930$, $\alpha = 1.925$, $\alpha = 1.810$.

for $\alpha = 1.925$ and $\alpha = 1.81$ behavior of $ReZ = ReZ(0, t)$ and $ImZ = ImZ(0, t)$ displays a disordered process that on the plane $(A, dA/dt)$ in Fig.3. reveals a structure similar to what is usually observed for stochastic attractors. Nevertheless, more specific statement needs more detailed analysis since our system is open and has many degrees of freedom.

In Fig.4., we show the spectrum of time oscillations of $Z(0, t)$ (see definition in Eq. (37)) for $\alpha = 1.940$, $\alpha = 1.930$, $\alpha = 1.925$, $\alpha = 1.810$. For $\alpha = 1.94$ and $\alpha = 1.93$, the spectrum has small numbers of harmonics, and it corresponds to the regime of synchronization in

the oscillator medium. For $\alpha = 1.925$, the spectrum is filled by additional harmonics. For $\alpha = 1.81$, the spectrum has a dense set of frequencies for the region $0.1 < \omega < 1$ that reflects the chaos behavior and turbulence of the oscillator medium. For the region $1 < \omega < 100$, we can see the integer power-law for the spectrum $S(\omega) \sim \omega^{-2}$ that corresponds to the main frequency dependence of equation (18).

VIII. TRAVELING WAVES AND BROADENING OF THE LIMIT CYCLE

Large number of oscillators and periodic boundary conditions permit to consider localized traveling waves (see for example for discrete systems in [30, 31]). Such waves were observed in our system (32) near the values of $\alpha \lesssim 2$ and disappear near $\alpha \approx 1$. In the latter case, it will be also demonstrated space-temporary localized topological defects.

The simulation was performed for the parameters

$$a = 1, \quad b = 0, \quad c = 2, \quad A_0 = 0.2. \quad (44)$$

For the value $b = 0$, the nonlinear term is real.

The waves propagation can be characterized by the group velocity $v_{\alpha,g} = \partial\omega_\alpha(K)/\partial K$. From Eq. (20), we obtain

$$v_{\alpha,g} = \alpha(c - b)g|K|^{\alpha-1}. \quad (45)$$

The phase velocity is

$$v_{\alpha,ph} = \omega_\alpha(K)/K = \frac{b - a}{K} + (c - b)g|K|^{\alpha-1}. \quad (46)$$

For the parameters used in the simulations we have $|v_{\alpha,g}| > |v_{\alpha,g}|$. In our simulation $K = 2\pi/64$. For our simulation $K = 2\pi/64$, and the decreasing of the order α leads to the increasing of the group and phase velocities.

The corresponding simulation is shown in Figs.5-8 for the surfaces $|Z_n(t)|^2$ (Fig.5), ReZ and ImZ plane (Fig.6), $(dA/dt, A)$ - plane (Fig.7) and spectrum $S(\omega)$ in Fig.8. Each of the the plate has the some additional information about solutions. There is a strong difference between values $\alpha = 1.99$, $\alpha = 1.45$, and $\alpha = 1.07$, $\alpha = 1.05$, $\alpha = 0.91$ while the case of $\alpha = 1.09$ is not clear since the finite time of simulation ($t < 1000$). The first case ($\alpha = 1.99$, $\alpha = 1.45$) shows traveling waves along x with regular (periodic or quasi-periodic) patterns.

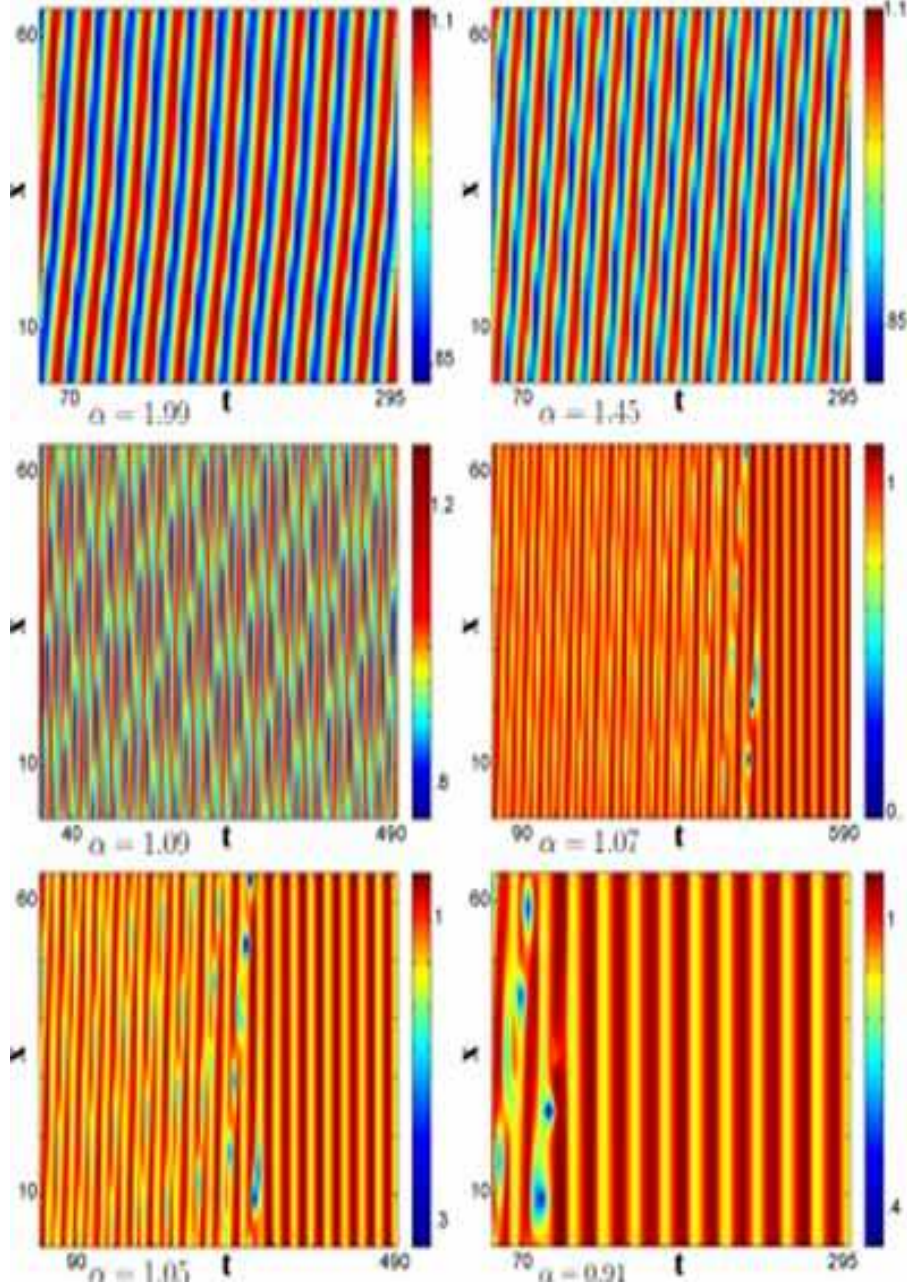


FIG. 5: Broadening of limit cycle. Wave front deinclination. Surfaces of $|Z_n(t)|^2$ vs t and $x = n$ for $\alpha = 1.99$, $\alpha = 1.45$, $\alpha = 1.09$, $\alpha = 1.07$, $\alpha = 1.05$, $\alpha = 0.91$. Simulations are realized for FGL equation with parameters $a = 1$, $b = 0$, $c = 2$, $A_0 = 0.2$.

In Figs 5,6, we observe the approach of the solution to a limit cycle with a few harmonics in the spectrum (Fig.8). At the same time the smaller is α , the smaller scales (larger values of K) enter the solution.

For α close to one ($\alpha = 1.07$, $\alpha = 1.05$, $\alpha = 0.91$) a fairly irregular pattern of traveling

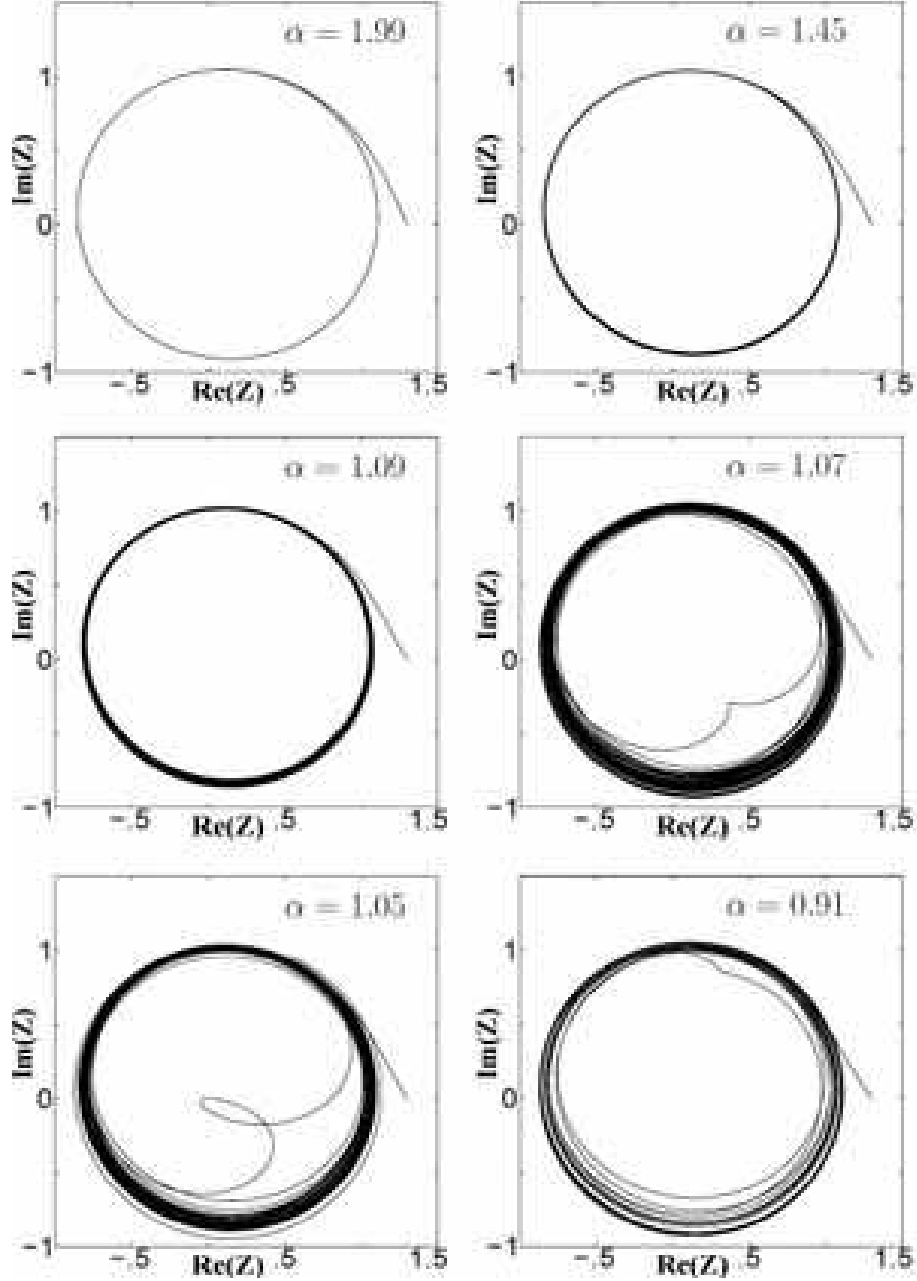


FIG. 6: Broadening of limit cycle. Plane $(Re\ Z, Im\ Z)$ shows projection of the complex amplitude $Z = Z(0, t)$ of the central oscillator as a function of time for $\alpha = 1.99$, $\alpha = 1.45$, $\alpha = 1.09$, $\alpha = 1.07$, $\alpha = 1.05$, $\alpha = 0.91$.

wave declines at some time, and synchronized oscillations take place. In the phase diagrams in Figs 6,7 a broadened limit cycle type picture corresponds to collective oscillations of the chain with fairly rich spectrum presented in Fig.8. The closer is α to one, the shorter is time of break of traveling waves, and the synchronized breather type solution appears. Since

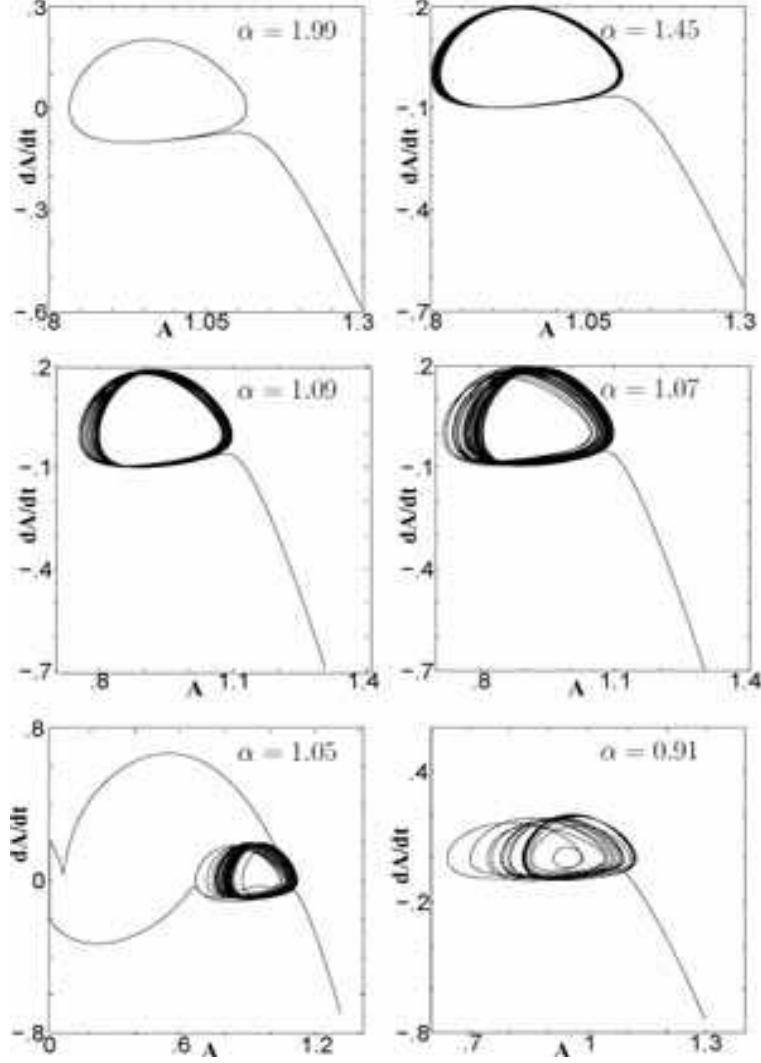


FIG. 7: Broadening of limit cycle. Appearance of topological defect. Plane $(A, dA/dt)$ shows projection of the trajectory of the central oscillator in phase space, where $A(t) = |Z(0, t)|^2$ for $\alpha = 1.99, \alpha = 1.45, \alpha = 1.09, \alpha = 1.07, \alpha = 1.05, \alpha = 0.91$.

the growth of wave numbers K of the solution, its amplitude can reach zero giving rise the topological defects [3]. Their appearance is clearly seen from Figs 6,7 for $\alpha = 1.05$ (see also Fig.5), when the amplitude $A(t) = |Z(0, t)|^2$ reaches zero value. It is seen that for $\alpha = 1.07$ and $\alpha = 0.91$ the dynamics is close to the appearance of the topological defect. Zero of the complex field Z result in singularity of the phase $\theta = \arg Z$. In two dimensions, points of singularities correspond to quantized vortices with topological charge

$$n = \frac{1}{2\pi} \oint_L \nabla \theta dl, \quad (47)$$

where L is a contour encircling a zero of Z .

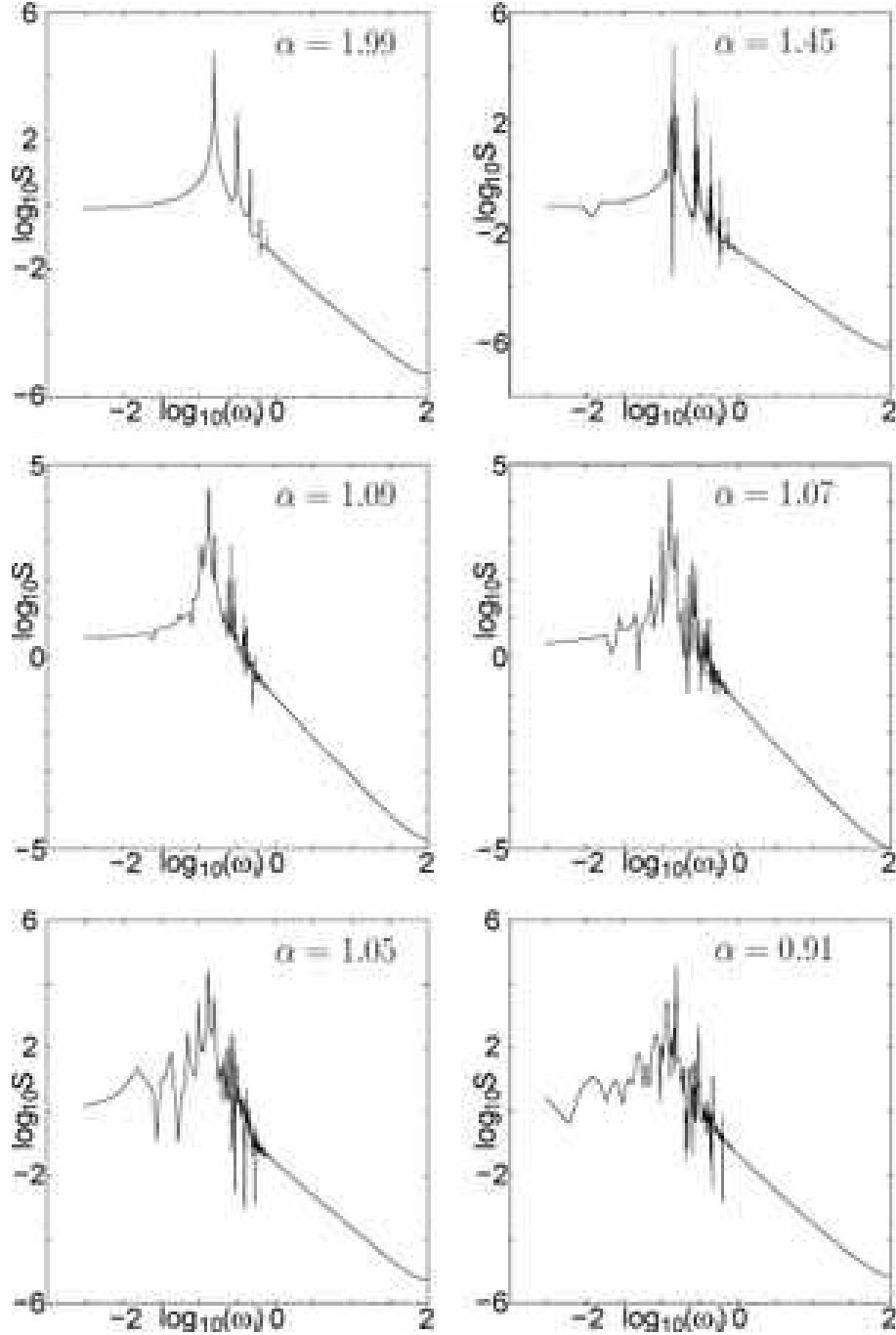


FIG. 8: Broadening of limit cycle. Spectrum of time oscillations of $Z(0, t)$ (see definition in Eq. (37)) for $\alpha = 1.99$, $\alpha = 1.45$, $\alpha = 1.09$, $\alpha = 1.07$, $\alpha = 1.05$, $\alpha = 0.91$.

For $1 < \alpha < 2$, we have the limit cycles around the point $A = 1$, $dA/dt = 0$. It is easy to see the broadening of these limit cycles, when α decreases.

Finally for this section, let us comment on the spectrum of time oscillations of $Z(0, t)$

for different α , presented in Fig.8. The broadening of limit cycle leads to widening of the spectrum. The spectrum is filled out by different harmonics that are localized in the region $0.1 < \omega < 1$. For $\omega > 1$, we have the dependence $S(\omega) \sim \omega^{-2}$ that follows directly from equation (14).

IX. AMPLITUDE DEPENDENCE OF THE TRANSITION TO TURBULENCE

In this section, we would like to show that the turbulent regime developing depends on the initial amplitude. For simulation, we use some parameters as in (41) [26] except of $\alpha = 1.45$.

It is seen from Fig.9, that the decreasing of the initial amplitude A_0 from 1.3 to 0.005 doesn't change, at least visually, the space-time structure of turbulence, but the change increases the time of developing an instability and beginning of turbulence. The turbulence possesses a robustness with respect to change of the amplitude of initial excitation and initial conditions.

In Fig.10., the plane $(A, dA/dt)$ shows projection of a trajectory of the central oscillator. There are random rotations on the plane and a broadening of the spectrum in a finite region of frequencies. The Fig. 10 shows many loops of the trajectory for which $dA/dt = 0$ and A is close to zero. That means that the turbulent regime includes many different points that are close to be the topological defects.

X. CONCLUSION

The main goal of this paper was to study influence of long-range interaction (LRI) on the developing of chaotic or turbulent motion in one-dimensional chain of large number of nonlinear oscillators. The LRI is characterized by the power of interaction α . In the continuous limit the corresponding equation is the nonstationary generalized Ginzburg-Landau (FGL) equation with complex coefficients and fractional derivatives of order α along the coordinate variables. Our preliminary research show different interesting regimes of behavior of the chain depending on the value of α . We have observed a synchronized motion of the chain with different complexifications such as defects, chaos, space-time turbulence,

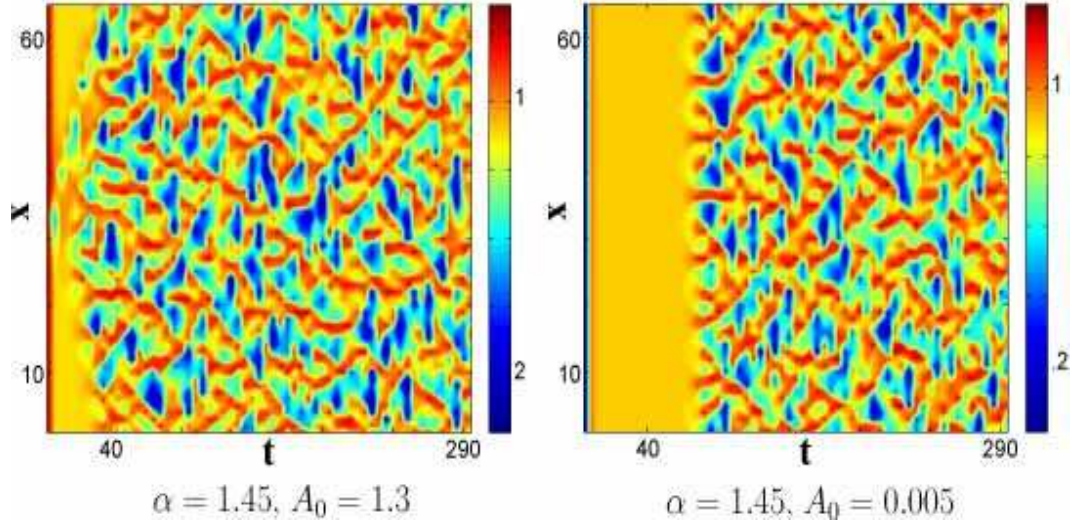


FIG. 9: Amplitude dependence of transition to turbulence. The decreasing of the initial amplitude from 1.3 to 0.005 gives that the space-time structure of turbulence almost is not changed. There is only increasing of time of beginning of turbulence.

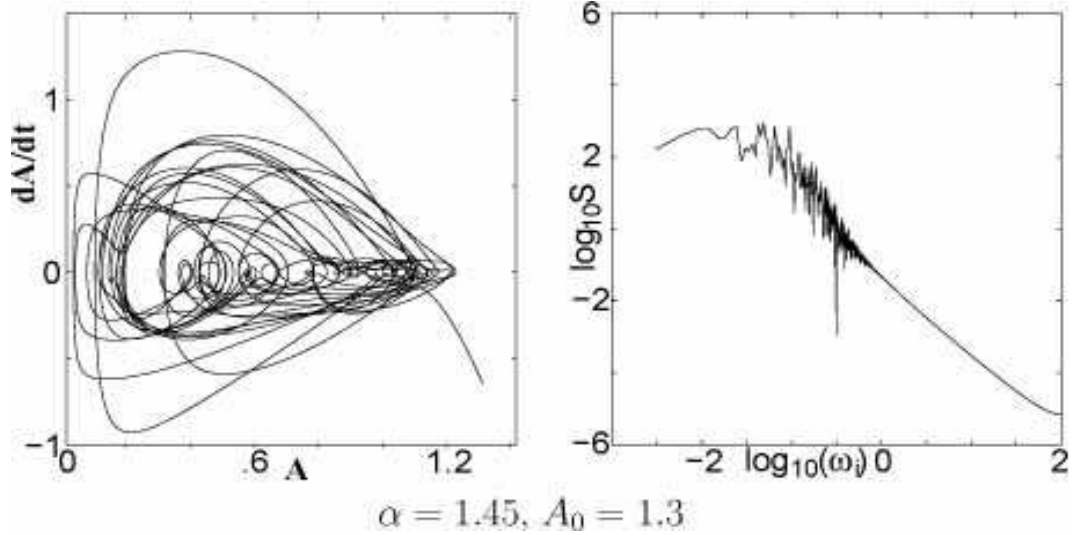


FIG. 10: Amplitude dependence of transition to turbulence. Plane $(A, dA/dt)$ shows projection of the trajectory of the central oscillator in phase space, where $A(t) = |Z(0, t)|^2$, and the spectrum of time oscillations of $Z(0, t)$ for $\alpha = 1.45$ and $A = 1.3$.

traveling waves. A possibility to use a continuous analog of the chain such as FGL equation, simplifies some estimates although it is well-known that discrete model is "more chaotic" than the continuous one.

Acknowledgments

This work was supported by the Office of Naval Research, Grant No. N00014-02-1-0056, and the NSF Grant No. DMS-0417800.

-
- [1] M.C. Cross, P.C. Hohenberg, Rev. Mod. Phys. **65**, 851 (1993).
 - [2] L.M. Pismen, *Vortices in Nonlinear Fields* (Oxford Science Publication, Oxford, 1999).
 - [3] I.S. Aranson, L. Kramer, Rev. Modern Phys. **74**, 99 (2002).
 - [4] D. Tanaka, Y. Kuramoto, Phys. Rev. E **68**, 026219 (2003).
 - [5] V. Casagrande, A.S. Mikhailov, Physica D **205**, 154 (2005).
 - [6] S. Shima, Y. Kuramoto, Phys. Rev. E **69**, 036213 (2004).
 - [7] Y. Kuramoto, D. Battogtokh, Nonlin. Phenom Compl. Syst. **5**, 380 (2002).
 - [8] Y. Kuramoto, *Chemical Oscillations, Waves, and Turbulence* (Springer, Berlin, 1984).
 - [9] A.T. Winfree, J. Theor. Biol. **16**, 15 (1967).
 - [10] F.J. Dyson, Comm. Math. Phys. **12**, 91, 212 (1969). Comm. Math. Phys. **21**, 269 (1971).
 - [11] M. Antoni, S. Ruffo, Phys. Rev. E **52**, 2361 (1995).
 - [12] C.J. Tessone, M. Cencini, A. Torcini, Phys. Rev. Lett. **97**, 224101 (2006).
 - [13] V.L. Pokrovsky, A. Virosztek, J. Phys. C **16**, 4513 (1983).
 - [14] C. Anteneodo, C. Tsallis, Phys. Rev. Lett. **80**, 5313 (1998).
 - [15] A. Pikovsky, M. Rosenblum, J. Kurths, *Synchronization. A Universal Concept in Nonlinear Sciences* (Cambridge University Press, Cambridge, 2001).
 - [16] S. Boccaletti, J. Kurths, G. Osipov, D.L. Valladares, C.S. Zhou, Phys. Rep. **366**, 1 (2002).
 - [17] V.E. Tarasov, G.M. Zaslavsky, Chaos **16**, 023110 (2006).
 - [18] N. Korabel, G.M. Zaslavsky, Physica A **378**, 223 (2007).
 - [19] H. Weitzner, G.M. Zaslavsky, Commun. Nonlin. Sci. and Numer. Simul. **8**, 273 (2003).
 - [20] A.J. Majda, D.W. McLaughlin, E.G. Tabak, J. Nonlin. Sciences **7**, 9 (1997).
 - [21] S. Flach, Phys. Rev. E **58**, R4116 (1998). A.V. Gorbach, S. Flach, Phys. Rev. E **72**, 056607 (2005).
 - [22] O.M. Braun, Y.S. Kivshar, Phys. Rep. **306**, 2 (1998).
 - [23] N. Laskin, G.M. Zaslavsky, Physica A **368**, 38 (2006).
 - [24] V.E. Tarasov, G.M. Zaslavsky, Physica A **383**, 291 (2007).
 - [25] A.A. Kilbas, H.M. Srivastava, J.J. Trujillo, *Theory and Application of Fractional Differential Equations* (Elsevier, Amsterdam, 2006).
 - [26] H. Chate, A. Pikovsky, O. Rudzick, Physica D **131**, 17 (1999).
 - [27] H. Chaté, Nonlinearity **7**, 185 (1994).
 - [28] M. van Hecke, Phys. Rev. Lett. **80**, 1896 (1998).
 - [29] A.S. Pikovsky, M.G. Rosenblum, J. Kurths, Int. J. Bifurc. Chaos **10**, 2291 (2000).
 - [30] G. Friesecke, Physica D **171**, 211 (2002).
 - [31] D. Treschev, Discrete and Contin. Dynam. Systems **11**, 867 (2004).